ACTIVE CONTOUR MODELS FOR SEMI-AUTOMATIC EXTRACTION OF FEATURES IN DIGITAL IMAGES

Eberhard Gülch
Department of Photogrammetry
The Royal Institute of Technology, Stockholm, Sweden

ABSTRACT

Active contour models, called snakes, are used to extract features in digital images in an interactive environment. The operator guides the deformable snake near the desired feature and the precise attraction is done automatically using energy minimization techniques. The solution is an optimal compromise between internal forces and external forces acting on the active contour model. The contour can include discontinuities of first and second order. Several implemented key point operators and their combination offer the possibility to lock the snake on a great variety of features in the image, like blobs, corners, terminations or edges. The technique is applicable for semi automatic photogrammetric mapping as well as for more automatical feature extraction in industrial applications. The snake technique offers an attractive link between high- and low-level visual interpretation with flexible degree of automation.

1. INTRODUCTION

One of the main reasons for introducing digital techniques into photogrammetry has been the possibilities of automating the measuring process. The research mainly concentrated on automation of the parallax measurement in digital stereo or multiple images. These methods are already very advanced and photogrammetric tasks like orientation, orthophoto and digital terrain model generation can be performed to a great extent automatically using techniques already in place /8/.

One of the main unsolved problems is the automation of feature extraction, which is also one of the most time consuming tasks in photogrammetric mapping. HELAVA /8/ and SCHENCK /13/ address the need to attack the problem of interpreting the model space by identifying objects and extracting features. MULAWA et al. /12/ are developing theories for the photogrammetric treatment of linear image features, leaving the point-field thinking. FÖRSTNER /4/ detects and locates houses in digital images as topographic control points using specific models. The working group 2 of ISPRS Comm. III is going to start activities on 'Object Reconstruction and Location by Image Analysis' and OEEPE Comm. F has initiated a test on 'Feature Based Segmentation'. New instruments have been developed by several companies during the last years and they have been used for several research projects already /2/,/14/. These fully digital photogrammetric stations offer the possibility to perform advanced image processing in a photogrammetric environment under the guidance of a human operator.

Other fields like computer vision are working already longer on the feature extraction problems. FUA et al. /6/ formulate a link between low-level and high-level image understanding by using model based geometric constraints to produce object delineations belonging to generic shape classes. HUERTAS et. al /9/ use generic models of the shapes to detect buildings in aerial images. LEBEGUE et. al. /11/ use 2-D and 3-D model based recognition for large man-made objects like highway bridges. ENGEL et al. /3/ are developping an interactive system for aerial photo interpretation in order to automate the extraction part.

In this context the Department of Photogrammetry at the Royal Institute of Technology has started a research project on 'A Semi-Automatic System for Object Description and Precise Localization in Digital Images'. In the application for photogrammetric map production the operator will keep the important role to conduct the mapping process. He will select the objects to be measured and classify them, but for the precise object localization he will be assisted by automatic procedures working in a multiple image environment. One part of the project consists of deriving desired features in a single digital image. Most often contours are to be measured, like road boundaries or the outline of houses. A technique called 'Active Contour Models' or 'Snakes' /10/ has been implemented to perform this task with a high degree of automation but possible interaction by operator.

This paper reports on the implementation and the first results with this technique. In chapter 2 the theory of the snakes will be presented. Chapter 3 describes the actual implementation and new extensions. In chapter 4 some empirical results are presented and discussed. Chapter 5 gives a summary and an outlook on the further development.

2. SNAKE-THEORY

In 1986 TERZOPOULOS /15/ reported on deformable models consisting of energy minimizing splines. In 1987 KASS et al./10/ presented the theory of active contour models. Because of the way the dynamic contours slither while minimizing their energy they called them SNAKES. Since then various researchers have used and developed further the snake technique for several purposes like e.g. feature extraction, computer animation, motion tracking or stereo matching. FUA et al. /7/ use it for an approach to automatically extract buildings and roads in aerial images. AMINI et al. /1/ introduced dynamic programming techniques for the minimization. ZUCKER et al. /16/ present an algorithm for inferring curves from images. Instead of seeking for one global curve, they synthesize a covering of the global curve consisting of a family of splines.

In the following the notation of KASS et al. /10/ is used to describe the theoretical background.

The behaviour of an active contour model (snake) is controlled by internal and external forces. The energy of a snake depends on where the snake is placed and how its shape changes locally in space. The active contour can be described in parametric representation:

$$v(s) = (x(s), y(s)) \qquad s = \text{arc length} \tag{1}$$

The snake attracts to features of an image structure by minimizing an integral measure which represents the snake's total energy. The energy functional is written as:

$$E^*_{snake} = \int_0^1 E_{snake}(v(s))\,ds = \int_0^1 E_{int}(v(s)) + E_{ext}(v(s))\,ds$$
$$= \int_0^1 E_{int}(v(s)) + E_{ima}(v(s)) + E_{con}(v(s))\,ds \tag{2}$$

The total energy is a sum of single energies, due to the fact that different forces can act on the active contour. During minimization the snake is deformed to find an optimal compromise between the constraints introduced by internal forces (E_{int}) and external forces (E_{ext}) consisting of image forces (E_{ima}) and external constraint forces (E_{con}).

2.1 Constraint Forces

2.1.1 Internal Forces

Internal forces open the possibility to introduce geometric constraints on the shape of the contour. The internal energy is composed of a first order term and a second order term forcing the active contour to act like a membrane or a thin plate:

$$E_{int}(s) = (\alpha(s) \, |v_s(s)|^2 + \beta(s) \, |v_{ss}(s)|^2)/2 \qquad (3)$$

It is assumed that a continous curve ties the contour points together. The tension is controlled by $\alpha(s)$ and the rigidity by $\beta(s)$. Position dependent parameters α and β allow the introduction of discontinuities in the contour. Setting $\alpha(i)=0$ and $\beta(i)=0$ allows a position discontinuity at point i. Setting $\beta(j)=0$ allows a orientation discontinuity at point j.

2.1.2 Image Forces

Image forces can attract the snake to salient features in the image. The image energy E_{ima} is written as a combination of different energy terms which are computed from the image $I(x,y)$. Lines, edges and terminations are used in the original version. By introducing a weight (w_k) to each energy functional (E_k) the total energy E_{ima} is a combination of weighted terms which provide a large variety of possible features which can be looked for.

$$E_{ima} = w_{line} E_{line} + w_{edge} E_{edge} + w_{term} E_{term} \qquad (4)$$

Line energy functional
The energy functional (5) is the intensity of the image itself. The snake can be attracted to dark or bright lines by using the sign of the weight to choose between bright and dark.

$$E_{line} = I(x,y) \qquad (5)$$

Edge energy functional
To find edges in the image a great variety of operators can be used. Here the snake is attracted to contours with large image gradients. To derive the gradients the image should be slightly smoothed. The energy functional is defined as:

$$E_{edge} = - | \nabla I(x,y) |^2 \qquad (6)$$

Termination energy functional
To find corners or terminations of lines or subjective contours the curvature of level contours in a Gaussian smoothed image C ($C(x,y) = G_\sigma(x,y) * I(x,y)$) is determined. The termination energy is:

$$E_{term} = \frac{C_{yy}C_x^2 - 2\,C_{xy}C_xC_y + C_{xx}C_y^2}{(C_x^2 + C_y^2)^{3/2}} \qquad (7)$$

2.1.3 External Constraint Forces

They are provided by higher level image interpretation or user-interface. The user selects starting points and can apply forces interactively on the snake during the minimization process. A

spring force can draw a snake to a desired position, a repulsion force can push a snake from one local minimum to the other.

2.2 Energy Minimization

The energy minimization is done in four steps. A variational integral is set up in the continous space, a pair of Euler equations is derived, the equations are discretized and solved iteratively until convergence.

$$E^*_{snake} = \int_0^1 E_{ext}(v(s)) + \frac{1}{2}\left(\alpha(s)|v_s(s)|^2 + \beta(s)|v_{ss}(s)|^2\right) ds \qquad (8)$$

The integrands of the variational integral (8) have the form $F(s,v_s,v_{ss})$. A function that minimizes the energy integral has to satisfy the following Euler equations:

$$F_v - \frac{\partial}{\partial s} F_{vs} + \frac{\partial^2}{\partial s^2} F_{vss} = 0 \qquad (9)$$

Substituting the corresponding terms yields the two independent Euler equations:

$$-\alpha x_{ss} + \beta x_{ssss} + \frac{\partial E_{ext}}{\partial x} = 0 \qquad (10)$$

$$-\alpha y_{ss} + \beta y_{ssss} + \frac{\partial E_{ext}}{\partial y} = 0 \qquad (11)$$

The Euler equations (10),(11) are discretized by approximating the derivatives by finite differences:

$$\begin{aligned} &\alpha_i(v_i - v_{i-1}) - \alpha_{i+1}(v_{i+1} - v_i) + \beta_{i-1}(v_{i-2} - 2v_{i-1} + v_i) \\ &- 2\beta_i(v_{i-1} - 2v_i + v_{i+1}) + \beta_{i+1}(v_i - 2v_{i+1} + v_{i+2}) + (f_x(i), f_y(i)) = 0 \end{aligned} \qquad (12)$$

with $v(0)=v(n)$ which means a closed contour and $f_x(i) = \frac{\partial E_{ext}}{\partial x_i}$ and $f_y(i) = \frac{\partial E_{ext}}{\partial y_i}$

The two discretized Euler equations can be written in matrix form

$$Ax + f_x(x,y) = 0 \qquad (13)$$

$$Ay + f_y(x,y) = 0 \qquad (14)$$

The position vectors are solved iteratively

$$x_t = (A + \gamma I)^{-1}(\gamma x_{t-1} - f_x(x_{t-1}, y_{t-1})) \qquad (15)$$

$$y_t = (A + \gamma I)^{-1}(\gamma y_{t-1} - f_y(x_{t-1}, y_{t-1})) \qquad (16)$$

with γ as a step size.

3. IMPLEMENTATION

The implementation is mainly based on the theory described in chapter 2. Some elements have not been used, like e.g. interaction during minimization. The internal forces are handled in a different way. Several new image forces have been added.

3.1 Constraint Forces

3.1.1 Internal Forces

In the actual version only closed contours are possible. The contour points need not to be equally spaced. The distance between adjacent points is taken into account in the approximation of derivatives by finite differences. The parameters α and β are kept fix for all points and they are set by operator. In addition they include a factor which weights the internal forces against the external forces.

3.1.2 Image Forces

In order to increase the number of features to which the Snake can attract other key point operators are introduced. The interestoperator as it is described in FÖRSTNER et al /6/ can be used to detect interesting points (*ipoi*), corners (*icor*) or centers of circles (*icir*) and also edge elements (*iedg*) in a two step procedure, the detection of optimal windows and the location of optimal points within the selected windows.

The total image energy is extended by four new terms:

$$E_{ima} = w_{line} E_{line} + w_{edge} E_{edge} + w_{term} E_{term} + w_{ipoi} E_{ipoi} + w_{icor} E_{icor} + w_{icir} E_{icir} + w_{iedg} E_{iedg} \quad (17)$$

a) Interesting points, corners and centers of circles

The first step consists in optimal window detection. The elements of the normal matrix N are computed in a window around each pixel using the gradient values g_r and g_c :

$$N = \begin{pmatrix} \sum g_r^2 & \sum g_r g_c \\ \sum g_r g_c & \sum g_c^2 \end{pmatrix} \quad (18)$$

The elements of the normal matrix N describe an error ellipse which gives a measure on the precision of the location. For distinct interesting points (*ipoi*), for corners (*icor*) and for centers of circles (*icir*) the error ellipse should be close to a circle and small. Two measures which can be easily derived from the matrix N without inversion are used to determine distinctness:

$$w = \operatorname{tr} N / \det N \quad (18) \qquad q = \operatorname{tr}^2 N / (4 \det N) \quad (19)$$

For each pixel (w) and (q) are computed. The roundness is described by (q) with a high value for round error ellipse. A small error ellipse results in a large (w). If (w) and (q) are larger than some thresholds, the window is regarded as optimal. A local non-maxima suppression is performed to separate selected windows.

Step two consists of point location by determining the optimal point within the selected windows. If large windows are used, the center of the optimal window can be still some pixels away from the optimal point within the window which describes the position of the feature best. The optimal point determination is done with subpixel precision in each selected optimal window.

For interesting points (*ipoi*) and corners (*icor*) the normal equations have the following form to derive the optimal point position (r_0, c_0) :

$$\begin{pmatrix} \sum g_r^2 & \sum g_r g_c \\ \sum g_r g_c & \sum g_c^2 \end{pmatrix} \begin{pmatrix} r_0 \\ c_0 \end{pmatrix} - \begin{pmatrix} \sum g_r^2\, r + \sum g_r g_c\, c \\ \sum g_r g_c\, r + \sum g_c^2\, c \end{pmatrix} \tag{20}$$

For centres of circles(*icir*) the normal equations are only slightly differnt:

$$\begin{pmatrix} \sum g_c^2 & -\sum g_r g_c \\ -\sum g_r g_c & \sum g_r^2 \end{pmatrix} \begin{pmatrix} r_0 \\ c_0 \end{pmatrix} - \begin{pmatrix} \sum g_c^2\, r - \sum g_r g_c\, c \\ -\sum g_r g_c\, r + \sum g_r^2\, c \end{pmatrix} \tag{21}$$

While seeking for interesting points and corners a statistical tests avoids the detection of centres of circles and vice versa. Up to now it is not possible to decide between interesting points (symmetrical feature) and corners (assymetrical feature), but by using both point type features of different size can be detected. A subpixel localization has greater advantages when the energy forces would be stored in subpixel resolution, at least locally around key points.

Energy functional
To introduce the information on the strength of an interesting point, all points in the window get an energy value. The optimal point gets the lowest energy. The energy is increasing to the borders of the window according to the distance or another measure. This is done because by filtering the energy values to determine the derivatives a single minimum at an interesting point could be smeared out and in addition the window supports the attraction of the snake to the optimal point itself.

b) Edge detection by Interest Operator

The roundness measure q (19) can be used to describe the likelihood of a point to be an edge. The error ellipse is elongated in the direction along the edge and small in the direction perpendicular to the edge direction. If q = 0 then one of the eigenvalues of the Normal Matrix N is 0 and the window lies on an ideal edge. In the same way as for interesting points, N, w and q are computed. For edges q must be lower than a threshold, w determines the strength of an edge. For edge detection mostly a 3x3 window is used. To get rid of too many edge pixels a non-maxima supression is performed to keep only strong edges.

Energy functional
The energy E_{iedg} is computed out of the roundness of the error ellipse and the size of the small axis. A subpixel detection which is also possible makes more sense when the energy forces are stored in subpixel resolution.

3.1.3 External Constraint Forces

Up to now only starting points are given interactively by operator. An interaction during minimization is not possible. An elimination and densification step for contour points avoids observed uncontrolled drifting and clustering of points along the curve in the original version. It avoids that points move on top of each other and it ensures an almost equal point distribution along the whole length of the contour.

3.2 Flow Chart

To give an overview on the described implementation Fig. 1 shows the essential parts of the programme in form of a flow chart.

The operator sets the following tuning parameters:

- contour point density
- weights α and β for internal forces
- maximal variation step
- convergency criteria
- weights for image forces
  [window sizes and thresholds for Interest Operator]
- filter sizes for smoothing

The operator gives the starting position of the contour via mouse interactively. The given contour points are densified and the internal forces of the contour are determined. The weigthed image energies are computed for the whole image or a filtered version and stored in a matrix of the same resolution as the image. If the same filtering is used for all iterations, this matrix has to be computed only once. At the contour point positions the external energy is interpolated.

In the relaxation process the new contour coordinates are derived and used to check for convergency. If it is reached the final contour coordinates are given. If a new iteration is needed then points are eliminated and/or densified and the internal and external forces computed again and introduced into a new relaxation step until convergence.

Figure 1: SNAKE - Implementation

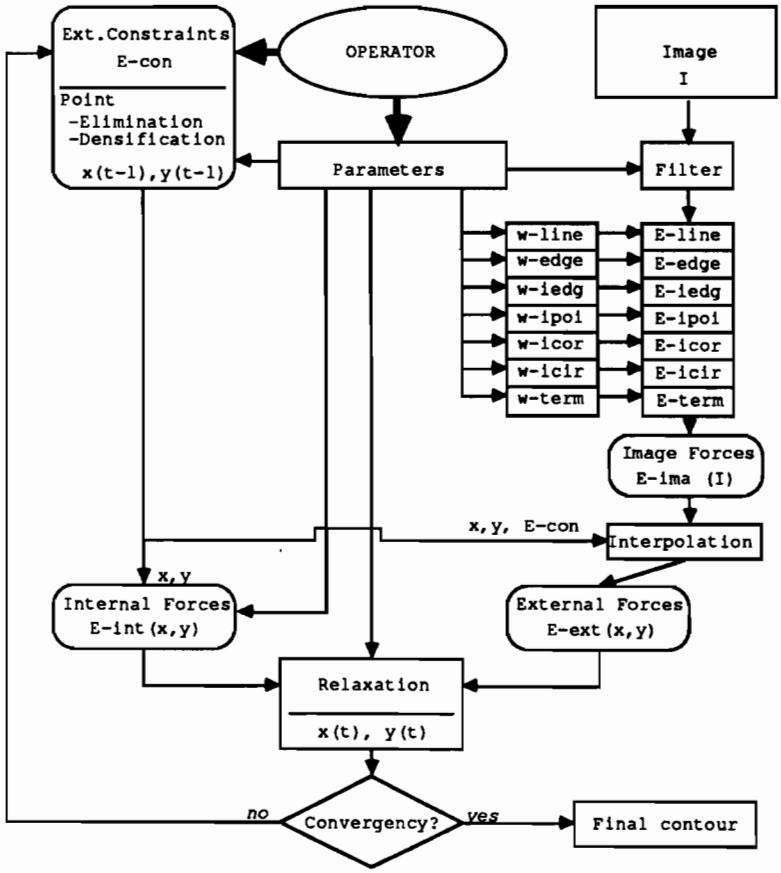

4. EMPIRICAL RESULTS

Four examples (Snake 1-Snake 4) shall demonstrate the results reached so far. Three different image patches are used (cf. Fig. 2-5). Images GRID 1 (64x64 pels) and GRID 2 (40x40 pels) are windows of a digital image taken by a CCD-Camera. They show a projected grid on a rough textured wooden cylinder. Image HOUSE (154x128 pels) is a 4 times reduced patch of a digitized aerial photograph and shows a single house in a garden. In all examples the actual snake position is overlayed as a polygon in **black** on the image. The image energy or single components are visualized as gray-value images with low energy values coded as **black**. Also on the energy images the snake position is overlayed in **black** or **white** for better comparison.

4.1 Snake 1

A first task is to find the black lines and the grid intersection points of one diamond in image GRID 1. The operator has given the initial position by 7 polygon points (Fig. 2a). The contour points are densified to 29 points (Fig. 2b). The image energies E_{line} (Fig. 2c) and E_{ipoi} (Fig. 2d) are applied to derive the total image energy (Fig. 2e). The varying, contracting contour from iteration 1 to iteration 25 is visualized in several steps through Figures 2 f)-k). The task is performed without single points of the snake drifting away along the adjacent black grid lines. This is due to the strong internal forces. The interestoperator provides the centres of the grid intersections to which the contour has locked on.

4.2 Snake 2

The second example shows two other image forces applied on image GRID 2 in order to measure the inner edge of a diamond. The initial contour is given by operator with 10 points (Fig. 3a) and densified to 16 points (Fig 3b). The image energy given in Fig. 3c) is a combination of E_{edge} and E_{icor}. After 21 iterations, visualized in several steps through Figures 3d)-i) the snake has expanded and attracted to the inner contour of the diamond.

4.3 Snake 3

Snake 3 used for the same task demonstrates what happens if only the edge energy E_{edge} is taken as image energy (Fig. 4a). The iterations 17 (Fig. 4b) and 21 (Fig. 4c) of Snake 3 are shown to directly compare them with the results of Snake 2 shown above. Snake 3 with the same initial position and the same parameters as Snake 2, except the type of image force, has attracted as well along the inner edges of the grid lines, but it didn't go into the two sharp corners to the left and to the right, but cut them off.

4.4 Snake 4

In example four the task is to attract to the border line of the roof of the building in image HOUSE. The operator has put the initial five points about 2-5 pixels away from the contour to be measured (Fig. 5a). After 81 iterations the snake has reached the position shown in Fig. 5b). This result has been achieved in the following way.

Close to the roof are areas with similar gray value and texture as the roof as well as a lot of edges and corners. Besides the roof two walls are visible and a large shadow area to the lower part. Straight through the roof and the middle of the patch goes the border line of two adjacent scan samples. There are a lot of traps the snake can fall in.

As image forces serve E_{line}, E_{edge} and E_{icor}. E_{line} (Fig. 5c) is used as the snake should attract to brighter gray values to support the staying on the roof as most of the background is darker. The main information is provided by the edges as it is visible in the edge energy image (Fig. 5d). But in some parts of the border no edges are found. In order to try to get the corners also the corner detector with a large window (9x9) is used (Fig. 5e). The total image energy with all weighted components included is shown in Fig. 5f). It can be expected that the snake would drift away on some of the critical points, therefore the internal forces are weighted strong compared to the external forces. The densified contour consists of 42 points at the beginning.

Figures 5g)-l) show several iterations during the minimization. The snake locks on very fast to the corners. The strong internal forces avoid that the snake drops off from the roof. They avoid that it follows the strong edge perpendicular to the upper border or jump over to the structure parallel to the lower left border (cf. Fig. 5f). After 41 iterations (Fig. 5k) the snake has attracted to all corners and all sides of the roof except to the middle of the upper border. Close by is some featureless gap, clearly visible in the energy image (Fig. 5f) from where no support is provided. 40 more iterations are performed to bridge this gap and correctly follow the outline of the upper border giving the satisfying result in Fig. 5b). The result is only checked visually by operator, no numerical comparison to check measurements in the analogue image is performed. Some of the corners could be represented more precise by a more dense point distribution close to such key points or a introduction of an orientation discontinuity at this points, which means variable parameters α and β. No corner point has been detected in the upper left corner (cf. Fig. 5e). This is due to the round corner caused by the low-pass filtering and the reduction of the original scanned image. In the original resolution the corner is more sharp and better detectable by the interest operator.

5. CONCLUSIONS

The active contour model technique in it's described version provides optimistic results. The snake expands and contracts to features of various type. The same mechanism is used to find edges, blobs, corners or other key points. The snake is able to bridge over photometrically weak boundaries because of the large support given by an integration of the information along the whole length of the active contour. Additional geometric constraints, like parallelity, or other image forces can be quite easily introduced as it is demonstrated by the interest operator.

A limited number of parameters is needed to steer the process. A main goal of further development is the automatic determination of some of the parameters and their time dependent changes. Parameters like window sizes or choice of image force could also be replaced by task, scale or feature dependent settings. These could be provided by a knowledge base, developed in another part of the research project. The parameters which control tension and rigidity must be variable in order to include discontinuities which can be quite easily introduced in the relaxation process. The main task is to detect them. The extension to open ended snakes is necessary to measure e.g. road boundaries. Scale space continuation and multiresolution in point density can speed up the convergency and enlarge the convergency range. This could also help to put the problem of approximate values more to the algorithmic side in order to concentrate the interaction on the minimization process, where often just a small push would be needed to let the snake finalize the contour.

A lack in theory up to know is an estimate of the quality of the result produced by the algorithm and suitable convergence criteria. In this context the planned OEEPE test can provide check data to analyse the quality and to compare the snake technique also with other approaches.

ACKNOWLEDGEMENTS

I would like to thank Prof. F. ACKERMANN who gave me the possibility to visit several institutes in the United States during my work at Stuttgart University which initialized my interest in the active contour models.

The support from the Department of Photogrammetry at the Royal Institute of Technology and the Swedish National Board for Technical Development (STU) is greatfully acknowledged.

REFERENCES

/1/ AMINI A.M. et al.: Using Dynamic Programming for Minimizing the Energy of Active Contours in the Presence of Hard Constraints, Proc. of the Second International Conference on Computer Vision, Tampa, Florida, USA, Dec. 1988

/2/ COGAN L.: KERN DSP1 Digital Stereo Photogrammetric System, Proc. of the 16th ISPRS Congress, Kyoto, Japan, 1988, Int´l Arch. Photogrammetry and Remote Sensing Vol. 27

/3/ ENGEL J.C., BOUTHEMY P.: A Query-Driven System for the Interpretation of Aerial Images, Proc. of the 6th Scand. Conference on Image Analysis, Oulu, Finland, 1989

/4/ FÖRSTNER W.: Model Based Detection and Location of Houses as Topographic Control Points in Digital Images, Proc. of the 16th ISPRS Congress, Kyoto, Japan, 1988, Int´l Arch. Photogrammetry and Remote Sensing Vol. 27, B10

/5/ FÖRSTNER W., GüLCH E.: A Fast Operator for Detection and Precise Location of Distinct Points, Corners and Centres of Circular Features, Proc. of the Intercommission Conference on Fast Processing of Photogrammetric Data, Interlaken 1987

/6/ FUA P., HANSON A.: Using Generic Geometric Models for Intelligent Shape Extraction, Proc. of the AAAI-87 6th National Conference on Artificial Intelligence, July 1987, Vol. 2

/7/ FUA P., LECLERC Y.G.: Model Driven Edge Detection, Technical Note SRI International

/8/ HELAVA U.V.: On System Concepts for Digital Automation, Proc. of the 16th ISPRS Congress, Kyoto, Japan, 1988, Int´l Arch. Photogrammetry and Remote Sensing, Vol. 27, B2

/9/ HUERTAS A., NEVATIA R.: Detecting Buildings in Aerial Images, Computer Vision, Graphics, And Image Processing, 41, pp.131-152, 1988

/10/ KASS M. et al.: Snakes: Active Contour Models, Proc. of the First International Conference on Computer Vision, London, England, June 8-11, 1987

/11/ LEBEGUE X.F. et al.: 2-D and 3-D Model Based Recognition of Man-Made Objects in Outdoor Scenes, Proc. of the 6th Scand. Conference on Image Analysis, Oulu, Finland, 1989

/12/ MULAWA D.C., MIKHAIL E.M.: Photogrammetric Treatment of Linear Features, Proc. of the 16th ISPRS Congress, Kyoto, Japan, 1988, Int´l Arch. Photogrammetry and Remote Sensing, Vol. 27, B10

/13/ SCHENK T.: The Effect of Digital Photogrammetry on Existing Photogrammetric Concepts, Procedures and Systems, Proc. of the 16th ISPRS Congress, Kyoto, Japan, 1988, Int´l Arch. Photogrammetry and Remote Sensing, Vol. 27, B9

/14/ STOKES J.: A Photogrammetric Monoplotter for Digital Map Revision using the Image Processing System GOP-300, Proc. of the 16th ISPRS Congress, Kyoto, Japan, 1988, Int´l Arch. Photogrammetry and Remote Sensing, Vol. 27, B2

/15/ TERZOPOULOS D.: On Matching Deformable Models To Images, Schlumberger Palo Alto Research Technical Report No.60, November 1986

/16/ ZUCKER S.W. et al.: The organization of Curve Detection: Coarse tangent fields and fine spline covering, in 'From Pixels to Features', J.C. SIMON (ed.), Elsevier Science Publishers B.V. (North Holland), 1989

Figure 2 a)-k): SNAKE 1 - Image GRID 1 (64 rows x 64 cols)

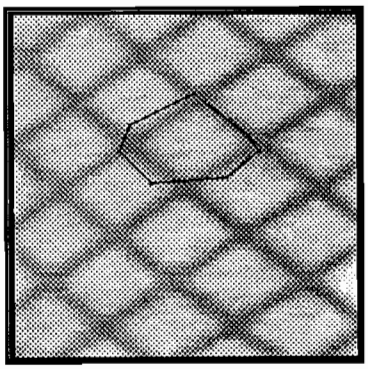

a) Snake 1-Initial Position

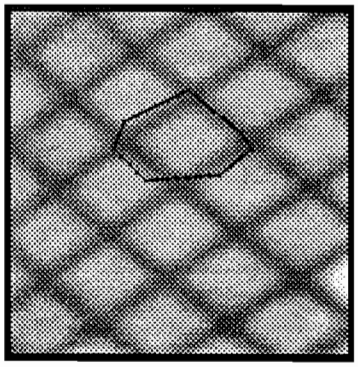

b) Snake 1-densified

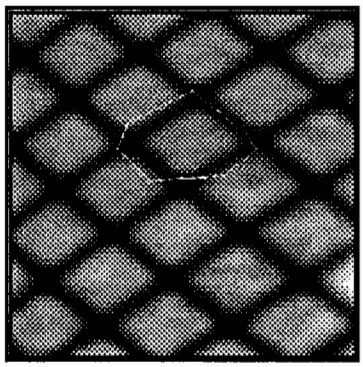

c) Image Energy (line)

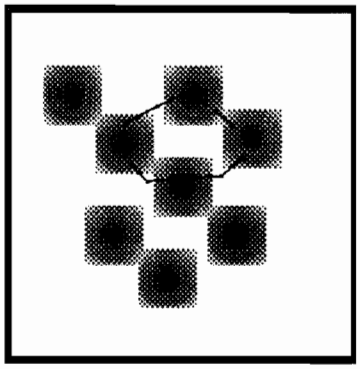

d) Image Energy (ipoi)

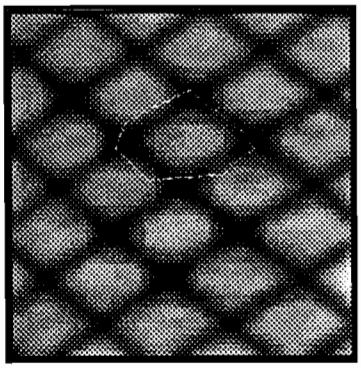

e) Image Energy (line,ipoi)

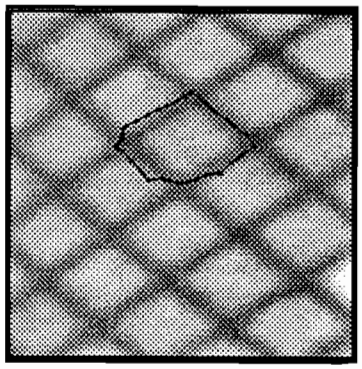

f) Snake 1-Iteration 5

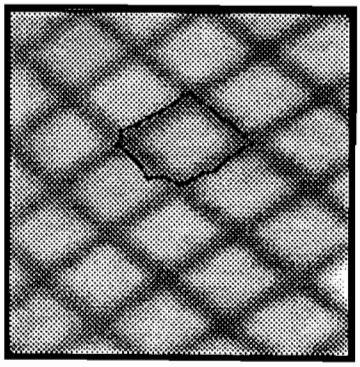

g) Snake 1-Iteration 9

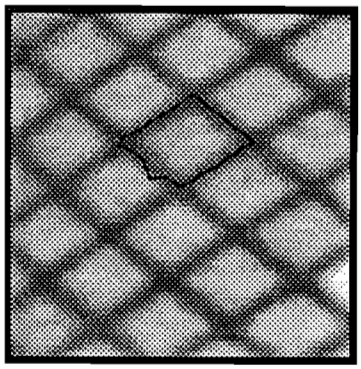

h) Snake 1-Iteration 13

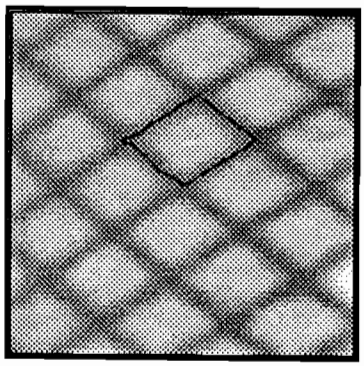

i) Snake 1-Iteration 17

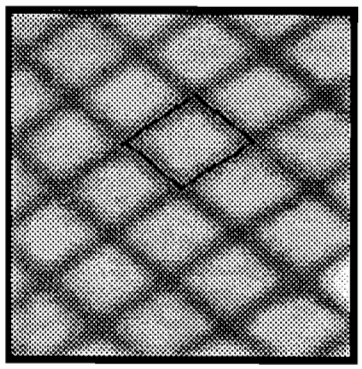

j) Snake 1-Iteration 21

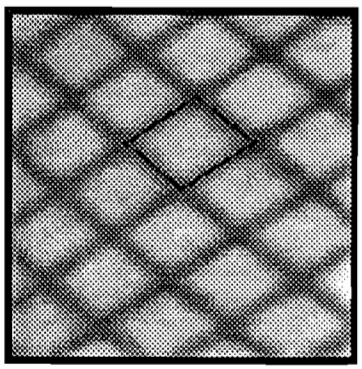

k) Snake 1-Iteration 25

Figure 3 a)-i): SNAKE 2 - Image GRID 2 (40 rows x 40 cols)

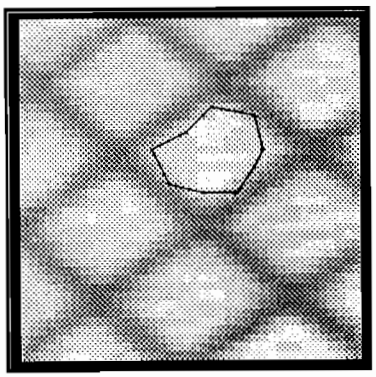

a) Snake 2-Initial Position

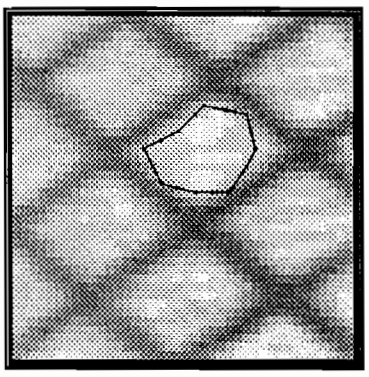

b) Snake 2-densified

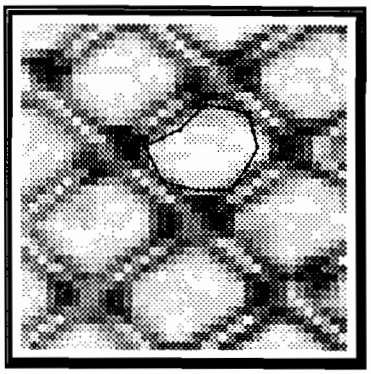

c) Image Energy (edge,icor)

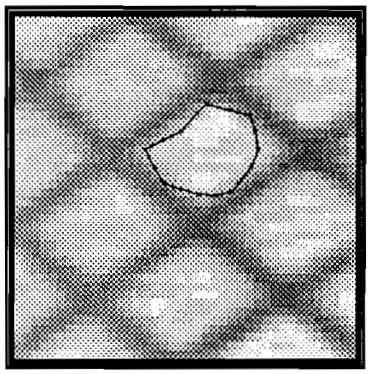

d) Snake 2-Iteration 1

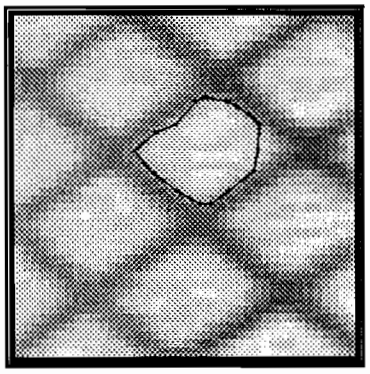

e) Snake 2-Iteration 5

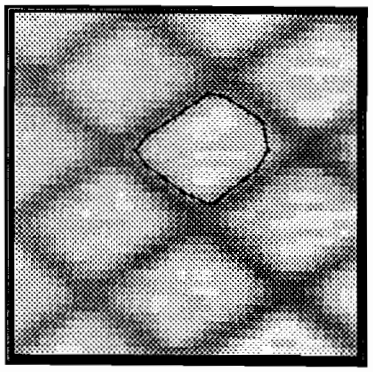

f) Snake 2-Iteration 9

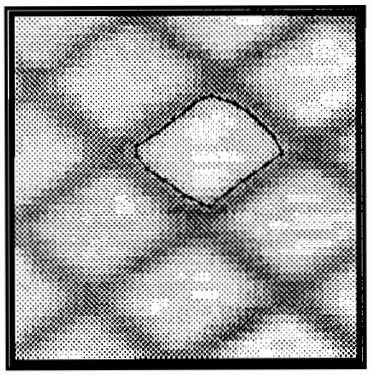

g) Snake 2-Iteration 13

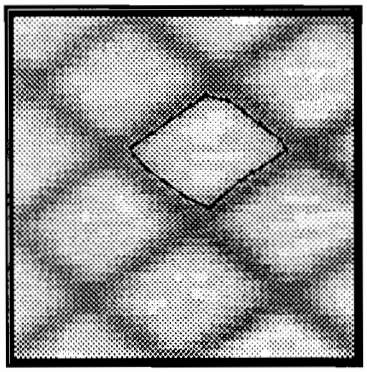

h) Snake 2-Iteration 17

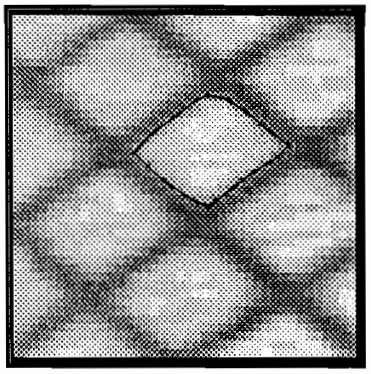

i) Snake 2-Iteration 21

Figure 4 a)-c): SNAKE 3 - Image GRID 2 (40 rows x 40 cols)

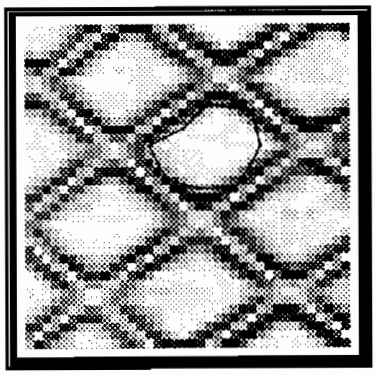

a) Image Energy (edge)

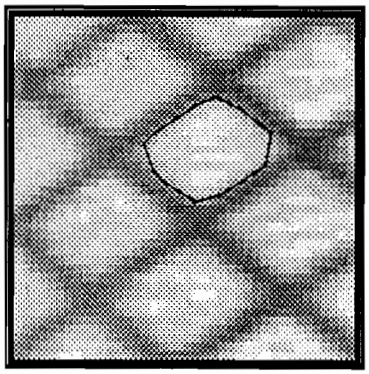

b) Snake 3-Iteration 17

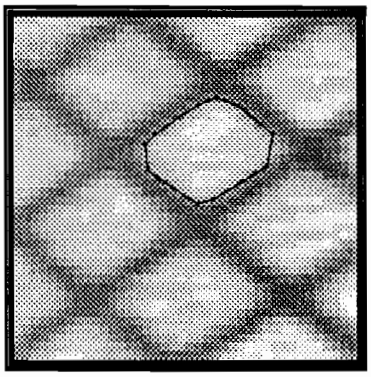

c) Snake 3-Iteration 21

Figure 5 a)-f): SNAKE 4 - Image HOUSE (154 rows x 128 cols)

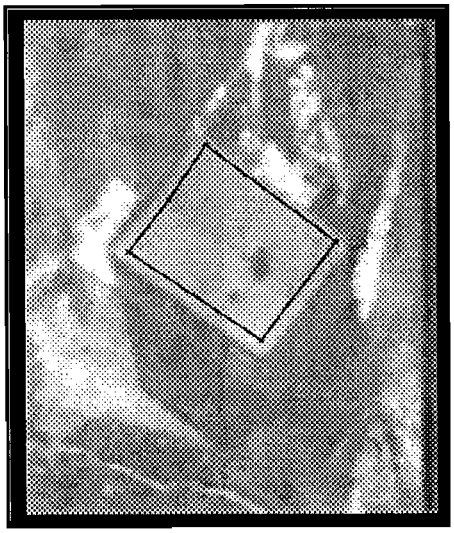

a) Snake 4-Initial Position

b) Snake 4-Iteration 81 (result)

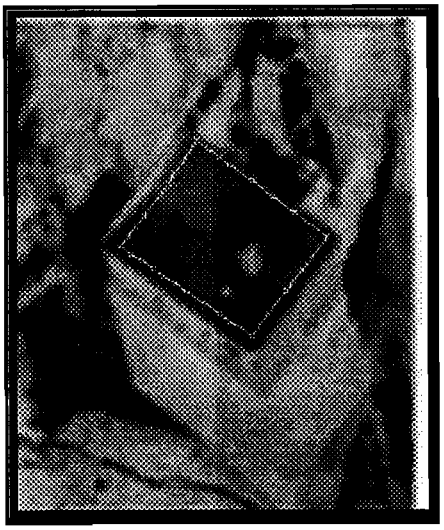

c) Image Energy (line)

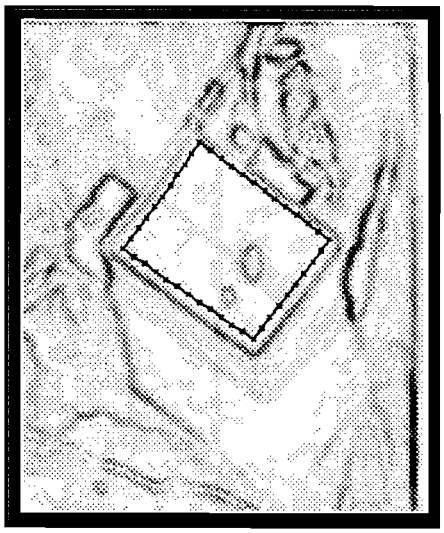

d) Image Energy (edge)

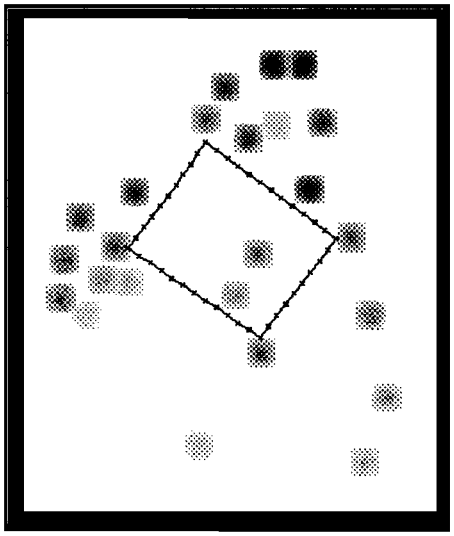

e) Image Energy (icor)

f) Image Energy (line,edge,icor)

Figure 5 g)-l): SNAKE 4 - Image HOUSE (154 rows x 128 cols)

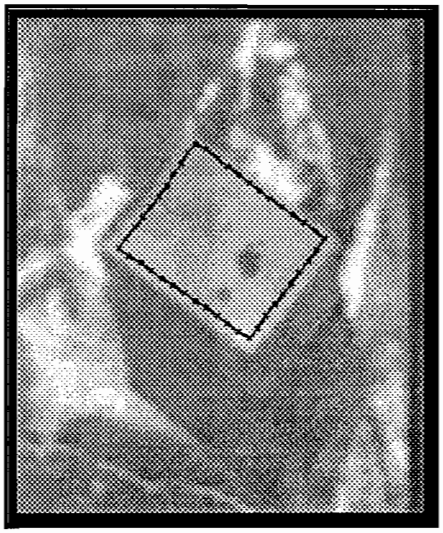

g) Snake 4-Iteration 1

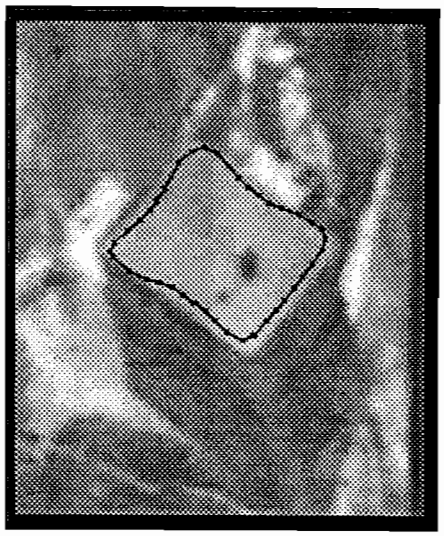

h) Snake 4-Iteration 11

i) Snake 4-Iteration 21

j) Snake 4-Iteration 31

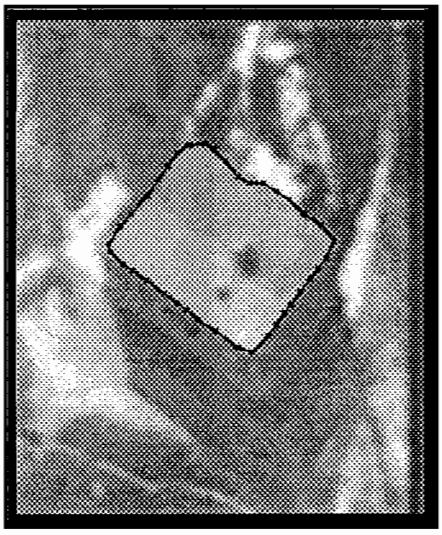

k) Snake 4-Iteration 41

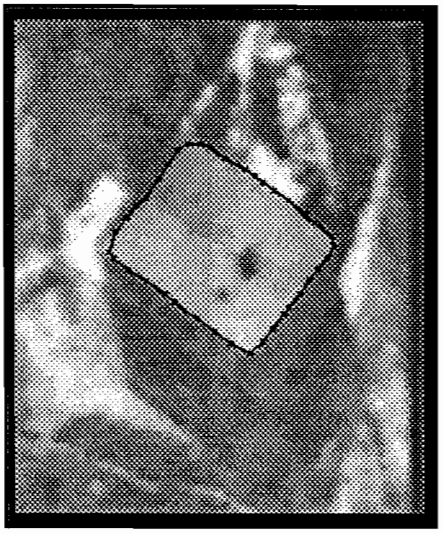

l) Snake 4-Iteration 61